

Military archaeology and LIDAR data visualizations: a non-invasive approach to detect historical remains

Joel Aldrighettoni¹, Maria Grazia D'Urso²

¹ Eng. Arch, PhD., Via L. Dalla Laita 16, 38061 ALA (Trento), Italy

² DISA, Department of Engineering and Applied Sciences, University of Bergamo, Viale G. Marconi 5, 24044 Dalmine (Bergamo), Italy

ABSTRACT

The present paper belongs to a line of research known as aerial archaeology and compares some specific visualizations of LIDAR data (hill-shading, openness, and sky view factor) to understand which of them can provide the best approach to suitably identify and unveil some archaeological permanences as function of different boundary conditions. In the present case, such permanences belong to the very special material heritage consisting of the "physical traces" of the Great War, although latent, they persist in the present landscapes at different states of preservation and visibility, waiting to be unearthed to express their cultural potential. They represent an indispensable palimpsest of "minor signs" such as, for example, fragments of entrenchments, gun emplacements, shelters, bomb craters, and temporary shelters. Such elements made the war machine work at that time while, nowadays, if properly recognized and enhanced, could foster the historical and cultural revitalization of the territories where they are placed.

Section: RESEARCH PAPER

Keywords: military archaeology; LIDAR; sky-view factor; Positive and Negative Openness; Great War heritage

Citation: Joel Aldrighettoni, Maria Grazia D'Urso, Military archaeology and LIDAR data visualizations: a non-invasive approach to detect historical remains, Acta IMEKO, vol. 12, no. 2, article 5, June 2023, identifier: IMEKO-ACTA-12 (2023)-02-05

Section Editor: Laura Fabbiano, Politecnico di Bari, Italy

Received November 13, 2022; **In final form** February 4, 2023; **Published** June 2023

Copyright: This is an open-access article distributed under the terms of the Creative Commons Attribution 3.0 License, which permits unrestricted use, distribution, and reproduction in any medium, provided the original author and source are credited.

Corresponding author: Maria Grazia D'Urso, e-mail: mariagrazia.durso@unibg.it

1. INTRODUCTION AND STATE OF THE ART

The morphological features of the land have always played a fundamental role in the perception of the landscape since they not only testify to changes in land use and land cover in relation to the needs of anthropogenic development, but also constitute the place where the "signs of history" have been imprinted and stratified. Therefore, being able to precisely know the topographic conformation of a territory means having a rich information potential at one's disposal that can prove useful in many application fields.

If in the past the study of the territory was essentially entrusted to the analysis of photographs from above taken from a bird's eye view during reconnaissance flights (particularly military aerial reconnaissance); conversely, in recent years, remote sensing techniques have evolved exponentially, thanks mainly to the continuous development of ever new tools and devices for spatial analysis and monitoring. From worldwide projects such as, for example, the Copernicus program with its satellites equipped with optical sensors and C-band synthetic aperture radar, to the accessibility of the GPS to an ever-

increasing number of users, from geotagging to online mapping applications, this is an innovative technological evolution [1]. The latter allows one not only faster and more systematic data acquisition, but also developing more specific interests in interferometric synthetic aperture radar (InSAR), airborne or ground-based laser scanning (ALS and TLS), unmanned aerial vehicle (UAV), automatic image matching, even through the use of thermal cameras, georadar, and other instrumentations [2]-[4]. As far as the acquisition of spatial datasets related to the actual morphological conformation of the territory is concerned, the Light Detection and Ranging (LIDAR) is the most commonly used technique for the creation of digital elevation models (DEMs), derived from the segmentation of point clouds obtained through measurements of the ground's distance from the laser emitter: each detected point is associated with a datum of geographic coordinates (according to the WGS84 system) and elevation calculated on the difference in time elapsed between the emitted and reflected pulse, and the intensity of the reflected signal itself [5]-[8].

Due to the possibility of integrating such remote sensing with RGB, hyper- and multispectral cameras, LIDAR data can provide multiple information useful in a variety of disciplinary

fields depending on the different visualization modes. Numerous studies focused on the study of these different ways of interpreting spatial datasets: Horkn et al. [9] mainly discussed the potential related to the visualization of shading as a useful tool for the elevation differentiation of surveyed features; Keith Challis et al. [10] began to study different techniques by proposing a "toolbox" that includes, in addition to shading, the study of ground slope and irradiance models; Hesse [11] specifically analysed the LRM (Local Relief Model); Yokoyama et al. [12] focused on the investigation of topographic aperture modes; Kokalj et al. [13] introduced the Sky view factor and its related applications for the analysis of soil microtopography (Relief Visualization Toolbox RVT - www.zrc-sazu.si/en/rvt).

From the study of the rich bibliography on this subject [14]-[22], it emerges that no single technique alone can extract the totality of the information contained in the source datasets, and therefore a proper combination of them is needed to make Digital Terrain Models (DTMs) "express" the best.

Concerning the contribution that these interpretations can provide in the archaeological field, it is also evident that not all techniques are equally useful since they vary in relation to boundary conditions such as, for example, the morphological nature of the context or the different conformation of the structures surveyed (concave or convex) [23].

Part of a long-started research [24]-[32], the work presented in this essay aims precisely at analysing and comparing some specific ways of visualizing LIDAR data to understand, first of all, which archaeological features they are able to highlight and whether their effectiveness varies according to the greater or lesser homogeneity of the input data (uniform or complex spatial morphologies). In this respect this contribution represents an extension of the paper entitled "Visualization of military heritage in the current landscape by comparing LIDAR features" presented at the Metroarchaeo2022 conference held in Cosenza, Italy in October 2022.

To better understand the operational effectiveness of the comparisons proposed in this paper, it is clearer to discuss the results by presenting the experiments that were conducted on specific study areas. The fortified territory of the Trentino-Tyrol Salient lends itself particularly well to this purpose as an archaeologically dense landscape of material remains deposited and stratified, more than a hundred years ago, by the First World Conflict. It is a "historical landscape of memory" on which the impact of the conflict was powerfully manifested by disseminating vestigia (not only forts but also barracks, trenches, shelters, and military infrastructure) that today, laden with memorial values, persist within the contemporary landscape to varying degrees of legibility, often "submerged" beneath additional layers deposited over time, waiting to be recognized and enhanced.

2. STUDY AREA AND DATA COLLECTION

In the European context of the 19th century the Austro-Hungarian monarchy fortified the entire area wedged between the Alps in defense of the southwestern borders with the construction of multiple defensive works [33]-[35]. These lines consisted of multiple permanent fortifications well connected by a dense network of temporary and field works conceived and designed to make the most of the orographic characteristics of the places (Figure 1). The implementation of the militarization plans, combined with the destructive impact that the conflict itself caused on the various territories, led to a radical

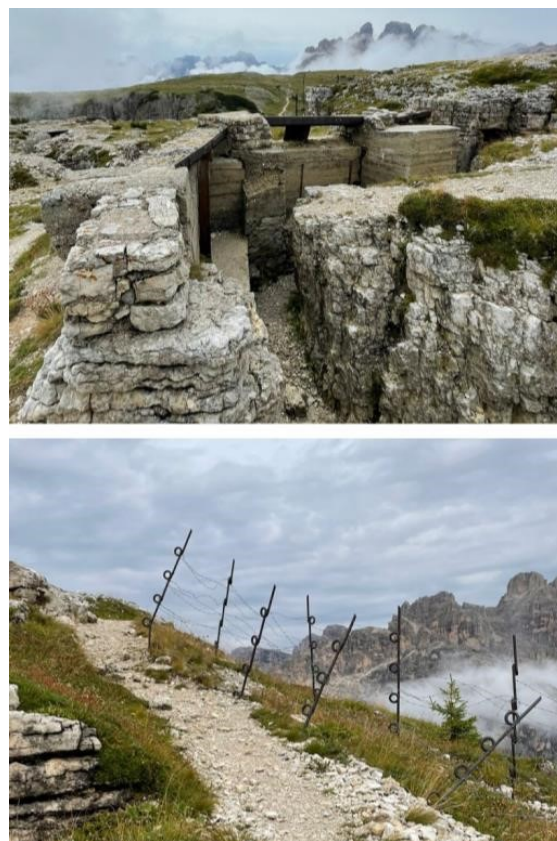


Figure 1. Monte Piana trenches (Trentino-Italy).

transformation of the overall landscape: on the Lavarone/Vezzena plateaus and on the southwestern front toward the Brescia area around Cima Rocca, in particular, the first phase of the war (1915-1916) was particularly violent and deeply disrupted the morphological conformation of those territories [36]-[40]. A hundred years after the end of the conflict, the current landscape still preserves some material traces of this part of history, but their recognizability is compromised by the state of degradation in which they are found and by the natural and anthropic transformations that have occurred over time. As can also be seen in many other "landscapes of memory" (in Figure 1, for example, the entrenchments on Monte Piana in Alto-Adige), in recent years concerned with the Great War heritage interventions have focused more on the permanent (more visible) fortifications, leaving in the background the minor vestigia, those "signs engraved" in the territory that are more fragile by nature and less identifiable but equally important and, therefore, to be recognized and preserved.

For these reasons, to facilitate these recognitions, it was decided to analyse these places through the comparison of different ways of visualizing LIDAR data to compare the results and understand their actual contribution to the recognition of these "latent signs" in the landscape; if rediscovered and enhanced, they could become an interesting driver of development for cultural tourism in these areas [41].

In particular, two sample areas with different morphological characteristics were compared: the mountain slope between Cima d'Oro and Cima Rocca on the ridge descending from the Ledro Valley to Garda Lake (Figure 2), which is characterized by unevenness and steep terrain, and the flat area of Vezzena around the "Basson position" (Figure 3), that, being a plateau, has no particular difference in elevation.



Figure 2. Entrenched systems between Cima d'Oro and Cima Rocca (Val di Ledro, Trento, Italy).



Figure 3. Fortified landscape of the Vezena Plateau, Basson position (Lavarone and Vezena Plateau, Trento, Italy).

Raw LIDAR data acquired by the Autonomous Province of Trento with remote sensing activities, dating back to the period between October 2006 and February 2008, were used for the analyses. These data were supplemented with other ASL surveys in 2014 and 2018, and now freely accessible and downloadable online in ascii-grid format with a 1×1 -meter cell grid, with a planimetric accuracy of $1/2000$ of flight altitude, and with an altimetric accuracy of approximately 15 cm.

3. METODOLOGY

The importance that LIDAR is increasingly assuming in the study of the dynamics of archaeological transformation of the landscape is foremost due to its ability to overcome the interference caused by the presence of vegetation. Indeed, in addition to the DSM, Digital Surface Model, which includes every surveyed element, LIDAR provides also the digital model of the orography of the terrain (the DTM, Digital Terrain Model), built exclusively with the points that belong to the ground. This is declined in the possibility of analysing the current topography of the territory in all its parts through a non-invasive and remote method, capable of overcoming the visibility limitations inherent in the study of single orthophotos (Figure 4). With regard to "war landscapes," in particular, the study of DTM makes it easier to identify the traces imprinted on the landform even in areas where land cover/land use has varied since the immediate post-war period, such as in newly planted forested settings (especially in mountainous areas).

However, the informative potential constituted by LIDAR data is greatly amplified by the implementation of advanced visualization modes (Hillshading, Sky View Factor, Openness) specifically developed for archaeological purposes and partially borrowed from other scientific fields, thus overcoming the traditional views of "grayscale" terrain elevation models, that avoid losing important archaeological features [42]-[44].

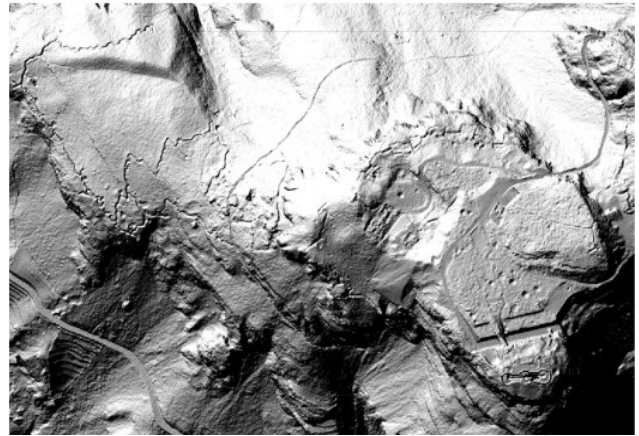


Figure 4. Pozzacchio Fortress and surroundings: orthophoto VS Hillshading visualization of Digital Terrain Model (DTM).

3.1. Analytical Hillshading and hillshading from multiple directions

Shading certainly represents the most common way of visualization of DTM obtained by LIDAR data elaboration as it returns a plastic and illustrative representation of ground topography that can be easily interpreted. As shown in Figure 5, the basic assumption is that the surface under analysis is illuminated by direct light from a fictitious light source placed at an infinite distance.

The algorithm calculates a reflectance value for each terrain pixel and is based on the Lambert's formula

$$E = \frac{I}{d^2} \cdot \cos \theta, \quad (1)$$

which postulates how this value is directly proportional to the light intensity I of the source S , the cosine of the angle θ between the direction of incidence and the normal to surface Δa , and inversely proportional to the square of the distance d between S

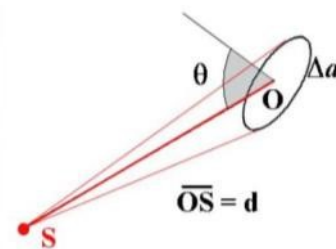


Figure 5. Illuminance calculation principle [9].

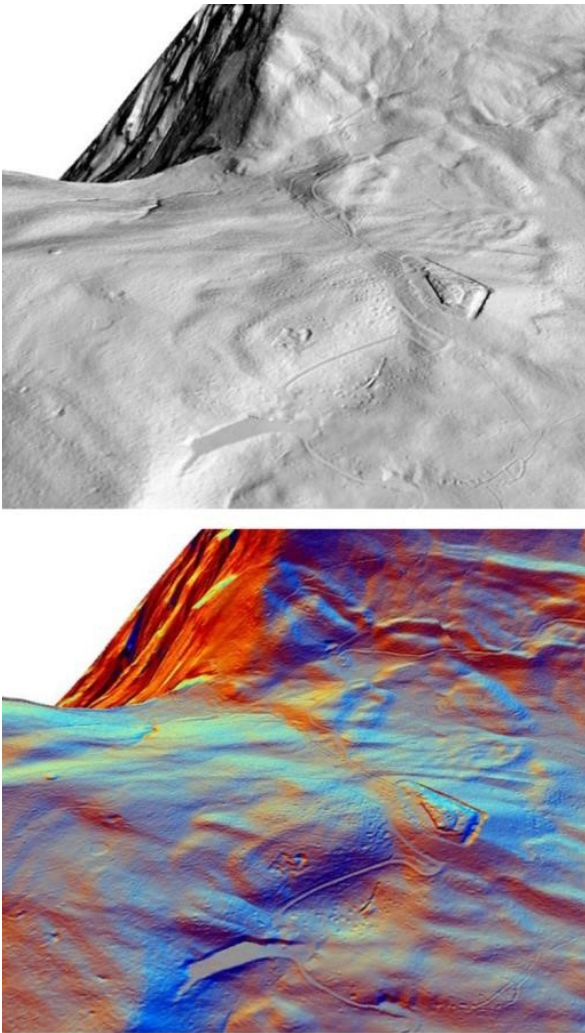


Figure 6. Vezzena Plateau: comparison between single Hillshading (above) and Hillshading from multiple directions (below) in RGB colour.

and $\Delta\alpha$. Areas invested perpendicularly to the light beam are the most illuminated ones, while areas with an angle of incidence equal to or greater than 90° are in shadow. The possibility of artificially setting such light source placements at any desired angle (even those not possible "in a realistic way") allows one to highlight even weakly signed features on the ground.

Since the colour change from white to grey and black enhances the perception of the relief morphology, the result of the algorithm is usually returned in grayscale, although this limits the visibility of fully illuminated or totally shaded areas. In addition, each specific direction of the illumination angles may be parallel to specific evidence on the ground that, when hit by a light beam in the same direction, would not become visible as they are shadowless. To overcome this problem, interesting hillshading from multiple directions algorithms have been proposed in the literature, i.e., applications of the analytical mode capable of mapping different hill shades with different but equally distributed angles between 0° and 360° on a single visualization, so as to simultaneously detect all the evidence on the ground. The most interesting visualizations are usually obtained by combining together between 8 and 16 directions, but the employed tool allows the user to manually choose the interval according to which spatial data should be analysed, depending on the degree of their definition and possible mutual interferences due to high autocorrelation. For the calculation of an 8-direction

visualization, for example, the preferred angles are equally distributed at regular intervals of 45° : 0° is always in band 1; 45° in band 2; 90° in band 3; up to 315° in band 8. Since the overlapping of multiple "grayscale" visualizations would not allow for a clear identification of the archaeological evidence, the proposed method suggests filtering the obtained processing to derive RGB images, since they are more immediately understandable. In this specific regard, the best settings consist of views implemented from three different directions, preferably at 60° intervals, which the different colour bands are associated with, for example, the red band at 315° , the green band at 15° , and 75° in the blue band. In this way we obtain raster images produced by the superimpositions of these three RGB layers concerning the shading obtained from the three chosen directions, on which other hillshading visualizations, chromatically graded accordingly, can also be appropriately combined. (Figure 6).

3.2. Sky-view factor visualization

A viable alternative to hillshading is the sky view factor analysis, achieved with an algorithm that simulates diffuse illumination on each DTM pixel coming homogeneously from all directions above, as if a uniformly illuminated hemisphere were above each point analysed and centred in it (Figure 7).

The SVF represents the measurement of the portion of the sky visible from each specific point on the surface; it corresponds to the measure of the solid angle calculated with the following analytical relationship:

$$\Omega = \sum_{i=1}^n \int_{\gamma_1}^{\pi/2} \cos \varphi \, d\varphi = 2 \pi \left(1 - \frac{\sum_{i=1}^n \sin \gamma_1}{n} \right), \quad (2)$$

in which φ corresponds to the latitude and λ to the longitude angle of the hemisphere, i.e. a function of the vertical elevation angle γ in the n directions of analysis. Normalizing the formula by 2π shows that, in the limiting cases, the formula returns a dimensionless parameter between 0 ($\gamma_1=90^\circ$, SVF=0, no visibility - black colour) and 1 ($\gamma_1=0^\circ$, SVF=1, all-clear view - white colour) that makes the irregularities of the terrain morphology obvious. In other words, values close to 1 indicate that the solid angle is near maximum, i.e., that the portion of

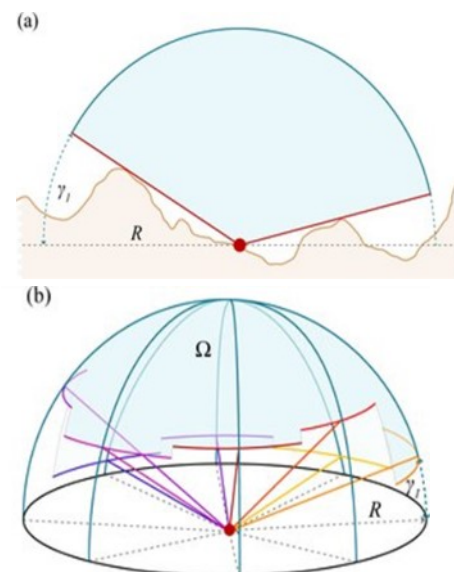


Figure 7. SVF calculation principle [13].



Figure 8. Serrada Fort: SVF visualization.

visible sky is large (in the case of flat surfaces or on the ridges of embankments), while near-zero values highlight the presence of depressions that reduce the amount of visible sky (in the case of deep valleys, incisions in the ground, cavities and pathways embedded in the ground).

The application of SVF for archaeological purposes in recognizing the permanence of Great War vestiges has revealed a rich palimpsest of "latent material signs," etched deep in the ground but otherwise barely visible, including entrenched paths and depressions with an almost circular pattern traceable to the negative interfaces produced by bomb explosions (Figure 8).

Briefly analysing in depth the variables of the computational algorithm, it becomes clear that the main factors influencing the outcome of SVF visualization are essentially the number of scanning directions and the maximum search radius. If the setting of the first parameter to 8, 16, 32, or 64 directions almost exclusively influences the accuracy of the definition of the edges of the detected objects, the choice of the maximum radius according to which to "scan" the microtopography depends on the scale of the features that will be detected. In other words: large survey features when a large search radius is chosen, and detailed features when a small radius is used. In the case study, for example, given the need to verify the permanence of remains of the minor vestiges of the Great War, a search radius estimated at about 5 m (10 pixels) was chosen to have a size comparable to that of the elements to be identified.

3.3. Positive and Negative Openness Visualization

Another way of visualizing LIDAR data is topographic aperture analysis, that aids the detection of surface concavities and convexities in a totally independent way of the presence/absence of a light source. Openness is a morphometric parameter defined as the average of several zenith or nadir angles (expressed in radians) within a predetermined horizontal distance (L) (Figure 9).

To obtain the aperture value for a given context, profiles along at least eight directions (N, NW, W, SW, S, SE, E, NE) within a defined radial distance must first be obtained from the DEM; hence, for each of them, the zenith angles:

$${}_D\phi_L = 90 - {}_D\beta_L \quad (3)$$

and nadir:

$${}_D\psi_L = 90 + {}_D\delta_L \quad (4)$$

can be determined [12].

The mean value of all zenith angles corresponds to the positive aperture, while the median of the nadir identifies the negative aperture. Being independent of the illumination factor, topographic openness highlights any morphological features of the terrain and the presence of both natural and artificial obstacles to the exclusion of general topographic information. As seen in Figure 10 in which openness was applied to an embankment with steep terrain slope, in both openness images, in fact, neither slopes nor shadows are shown, but for each point the maximum aperture value with respect to zenith (positive-light values) or nadir (negative-dark values) is returned, and not with respect to a hemispherical canopy horizontally centred at the point itself as in the SVF calculation. As demonstrated by application to the case study, this will be particularly advantageous in the recognition of archaeological evidence in areas where the slope of the terrain is particularly steep.

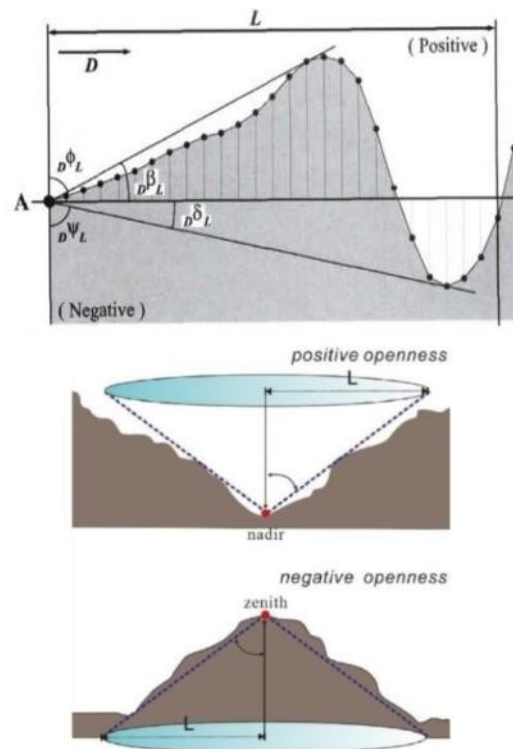


Figure 9. Principle of calculation Openness [12].

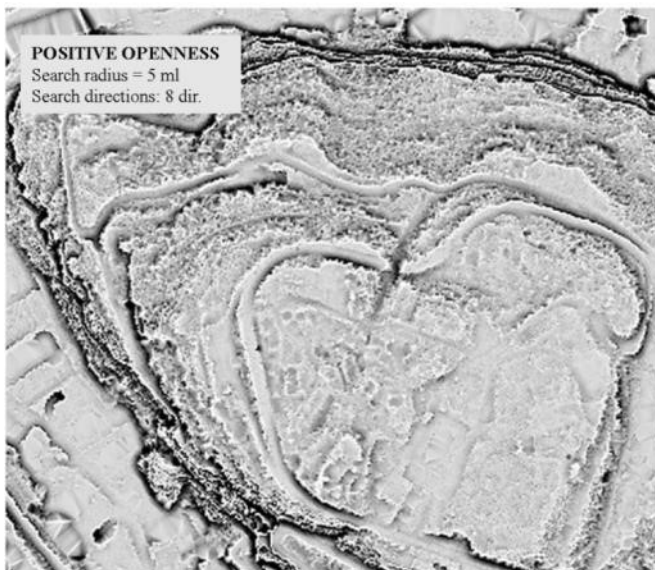
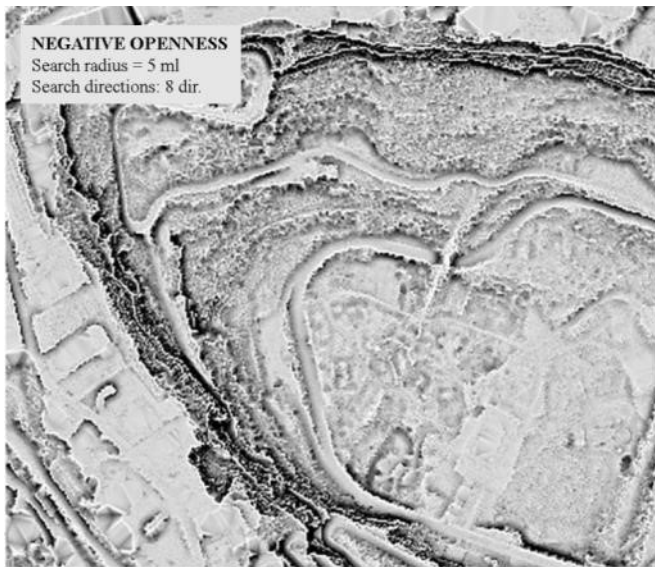


Figure 10. Positive (above) and Negative (below) Openness.

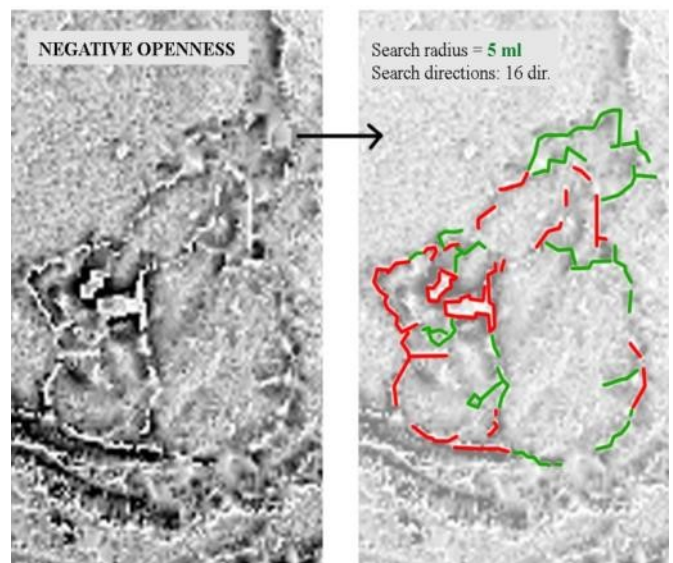
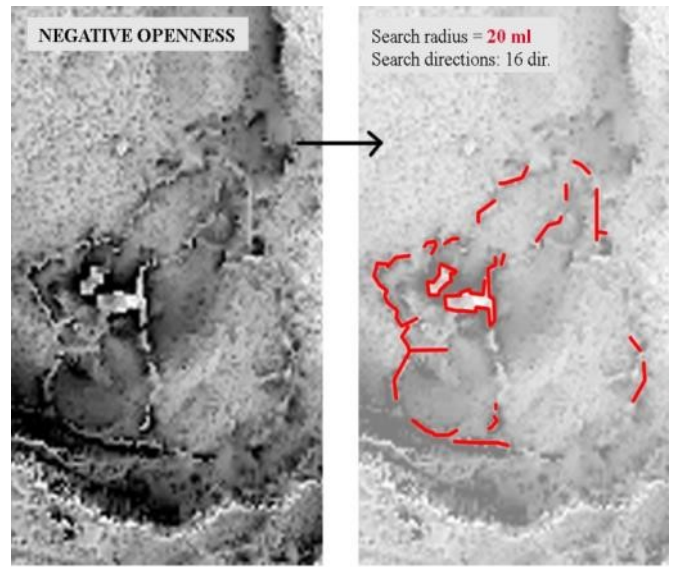


Figure 11. Search radius accuracy: comparison of the results.

As with the SVF, the accuracy of visualization is a function of the number of analysis directions (usually 8 or 16 directions) and of the maximum search radius. Indeed, as it can be seen in Figure 11 in which this visualization is applied on a multi-layered landscape having a dimensionally small archaeological evidence to be identified (around 1-5 linear meters), if the search radius settings are very different from this definition (around 15-20 pixels) the resulting processing is not sharp and, therefore, only some of the existing archaeological evidence (drawn with red lines) can be recognized. On the contrary, if the analysis radius is dimensionally similar to the surveyed objects, openness succeeds in highlighting many more "historical signs" (indicated in green colour) with greater accuracy for both geometric edges and depths.

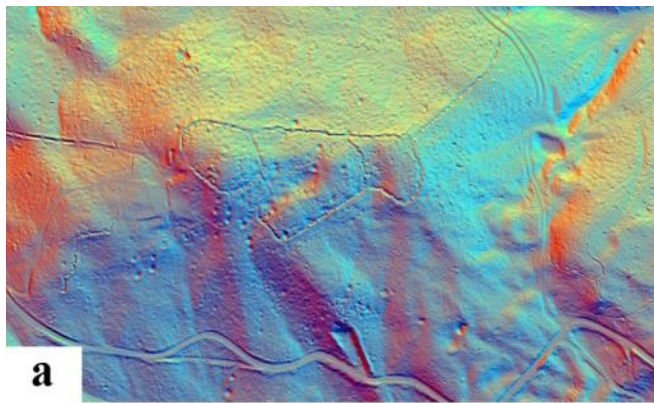
4. RESULTS AND DISCUSSION

As shown in Figure 12 and Figure 13, the different visualizations on the fortified surroundings of Cima d'Oro/Cima Rocca and of the "Basson position" on the Vezzena Plateau made it possible to identify, with centimetre precision, the microtopography of these historical landscapes revealing numerous concavities of almost circular shape and long

depressions in the ground with a more linear trend. Using 8 analysis' directions and calibrating the maximum scanning radius of 5 meters (10 pixels), i.e., a dimension compatible with the dimensions indicated in military manuals regarding entrenchments and gun emplacements, the identified irregularities turned out to be precisely the "physical signs" related to what remains of the imprint left by the Great War more than a century ago.

Analysing the obtained elaborations, it is immediately evident how the visualizations concerning the flat context around the "Basson position" appear more immediately understandable. In fact, the local morphology of the area is more homogeneous and consequently also the identification of some of the existing irregularities is already possible through the shading of the DTM (Figure 12a).

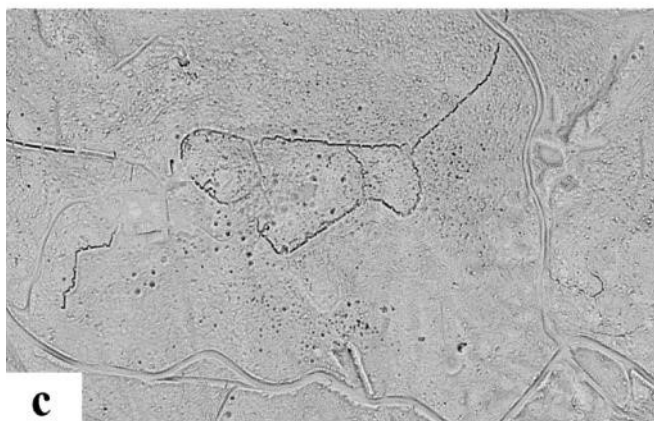
However, the SVF and topographic aperture provide more interesting data for a more precise definition of the geometric features of such "signs", especially concerning the sharpness of edges, the configuration of convex elements, and the relative depth of depressions, which can be identified with gray-scale displays where black corresponds to greater depth and white to maximum exposure (Figure 12b-c-d).



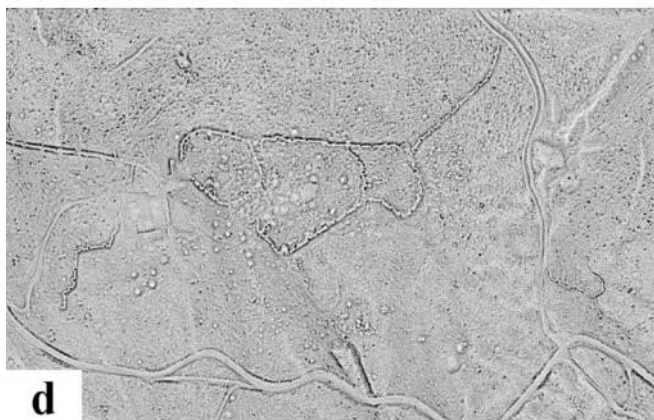
a



b



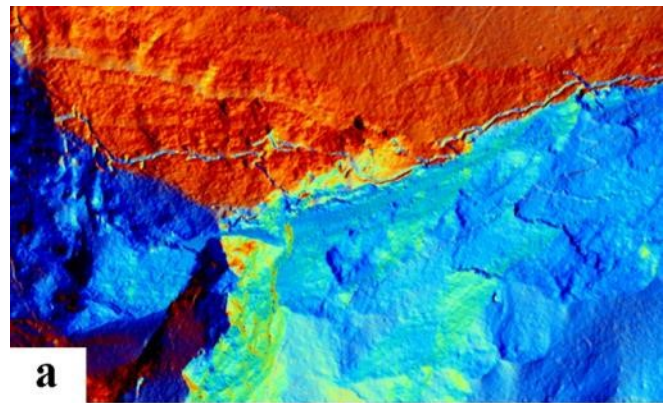
c



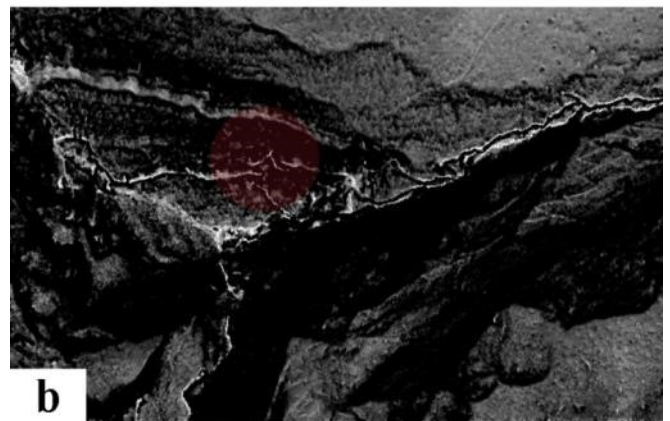
d

Figure 12. "Basson position" on the Vezzena Plateau (lowland context), Lidar data visualizations comparison:

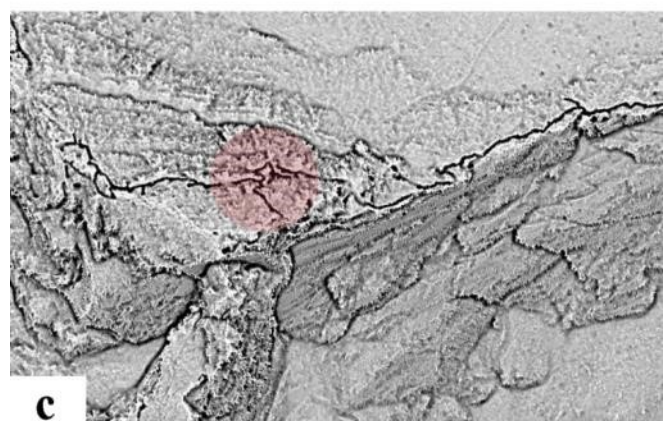
- a. Hillshading from multiple directions;
- b. Sky-view factor (8 directions – 5ml max radius);
- c. Positive Openness (8 directions – 5ml max radius);
- d. Negative Openness (8 directions – 5ml max radius).



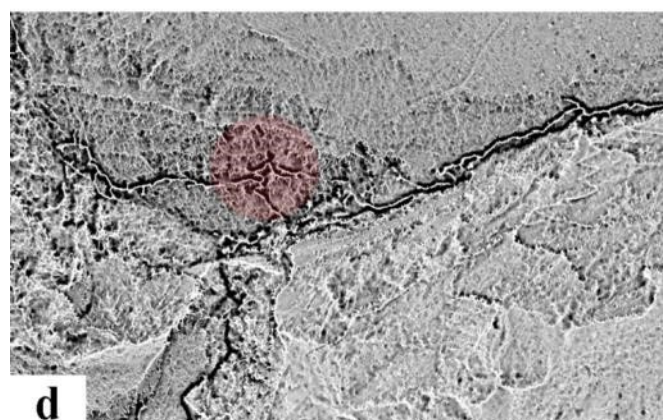
a



b



c



d

Figure 13. Cima d'Oro/Cima Rocca fortified positions (mountain context), Lidar data visualizations comparison:

- a. Hillshading from multiple directions;
- b. Sky-view factor (8 directions – 5ml max radius);
- c. Positive Openness (8 directions – 5ml max radius);
- d. Negative Openness (8 directions – 5ml max radius).

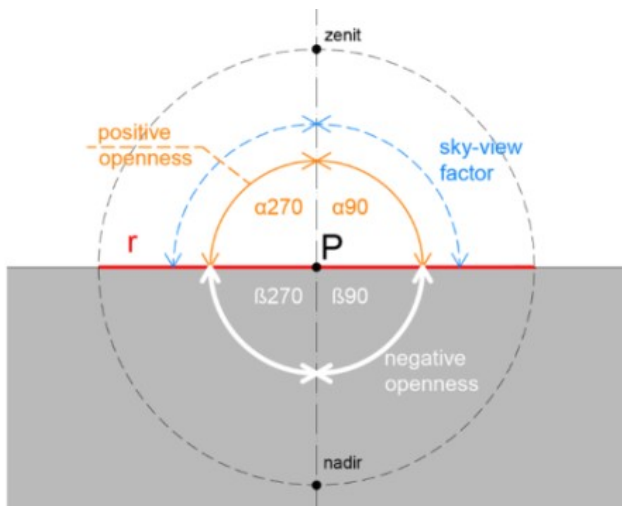


Figure 14. SVF VS Openness – sloping context.

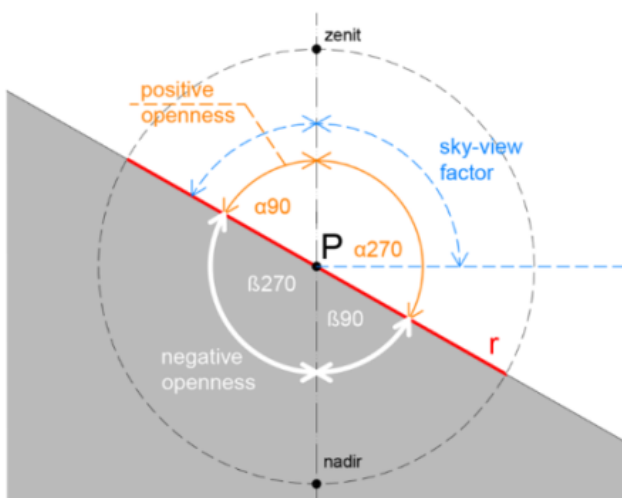


Figure 15. SVF VS Openness – lowland context.

On the other hand, as far as the mountainous area is concerned, the shaded visualization facilitates the understanding of the degree of terrain slope and highlights only the most markedly incised paths in the terrain (main roads), but it is not equally effective for the recognition of "minor" signs imprinted in the local microtopography. Analysing Figure 13b is evident that even SVF makes only a partial contribution because the visualization of the results obtained by the algorithm is largely influenced by the degree of terrain slope (dark part) that limits the visible portion of the sky.

Therefore, the most suitable visualization is the topographic aperture, which allows for the accurate detection of archaeological remains even in areas where shading and SVF are not particularly useful. This becomes clear by comparing Figure 13c/d with Figure 13a/b. This simple comparison is not only related to the analyzed case study, but it also allows to understand potentials and criticalities of different LIDAR data visualizations in relation to the type of morphological context of reference. Specifically, the reasons for the greater readability provided by the topographic aperture versus SVF (Figure 13) stem directly from the setting of the computational algorithm underlying the respective visualizations. Indeed, as is evident in Figure 14 and Figure 15, the SVF uses only the zenith angles above a fictitious horizontal plane centred on the point under analysis. Therefore, the maximum angle derived during

processing cannot be larger than a hemisphere (zenith of 90°). On the contrary, topographic aperture also includes angles of larger amplitude. In other words, this means that positive and negative aperture does not consider the slope factor, returning the same value regardless of whether it was determined on a horizontal (Figure 14) or inclined (Figure 15) surface. Although this reduces the understanding of overall topography, sharper views of topographic structures are obtained, not masked by slope values as in the SVF. Therefore, it can be seen that while in flat contexts SVF and topographic openness essentially provide comparable results (at least with respect to concave elements), in mountainous contexts where slope values are considerable, topographic openness provides a more significant contribution to the recognition archaeological remains.

Confirming the above, thanks to openness, it was possible to "scan" in detail the topography of the sloping slope between Cima d'Oro and Cima Rocca, thus identifying some convex elements and depressions that, without this analysis, could not have been recognized. Thanks to the precise location of such "signs," it was possible to carry out an inspection and validate what emerged from the remote analysis. As it can be seen in Figure 16, the surveyed elements were recognized as fragments of drystone walls supporting the defensive position (Vn1-a), while the linear depressions coincided with the entrenched paths that connected the two mountain peaks (red point in Figure 13 for the localization).

Finally, for areas where archaeological remains of vestiges have emerged, the use of DTM has also made it possible to derive punctual spatial sections that, in the case of entrenchments and other works built for the war, could be compared with specific design drawings or typological-constructive references found in military manuals. This represented an additional interesting comparison to better recognize the thickness of the ground that buried the vestigia in the last century, hiding them from view but preserving their testimonial value (Figure 17). At the operational level, since we are dealing with "in depth" analysis, SVF and Negative Openness represent the most appropriate visualizations able to locate the areas from which the sections can be derived. As already pointed out, this facilitates the reading of the concavities of the terrain.

5. CONCLUSIONS

It is evident how the interpretation of different ways of visualizing LIDAR data constitutes an important methodological contribution useful in unveling the constituent plots of the



Figure 16. Defensive position Cima d'Oro.

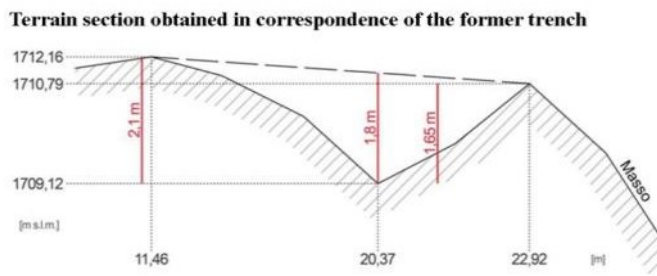
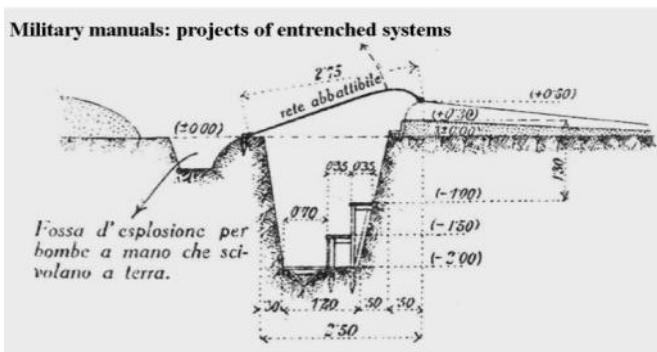
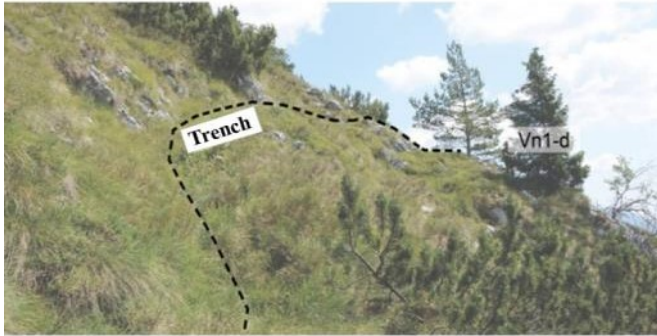
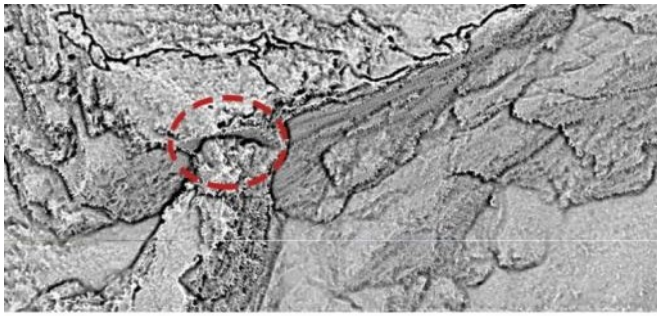


Figure 17. From remote analysis to in situ detection: the contribute of territorial sections to understand the depth of the vestigia permanences.

evolutionary biography of contemporary landscapes. The experimentation on the two study cases made it possible to unveil what remains of the pregnant cultural heritage related to the Great War and, at the same time, to compare the different visualizations to understand their potentials and criticalities at a general level.

In summary, it emerged how shading from multiple directions is valid for essentially getting a general view but not for specific analyses of local microtopography, with respect to which the contributions of SVF and topographic aperture perform much better. It was also understood how the main criticality of SVF is related to the incidence of terrain slope values that alter the visualization of results thus leading to a preference, for mountainous contexts, for the visualization of topographic

aperture as the main tool for the rapid identification of archaeological features.

Ultimately, a careful combination of SVF (which considers general topography) and topographic aperture (focused on differences in micro-relief) represents an essential operational contribution that facilitates the legibility of historical permanences in present-day landscapes, also opening up future research developments, such as, for example, the implementation of semi-automatic recognition and classification processes of archaeological evidence.

REFERENCES

- [1] I. Ali, S. Cao, V. Naeimi, C. Paulik, W. Wagner, Methods to Remove the Border Noise From Sentinel-1 Synthetic Aperture Radar Data: Implications and Importance For Time-Series Analysis, *IEEE Journal of Selected Topics in Applied Earth Observations and Remote Sensing* 11(3) (2018), pp. 777-786. DOI: [10.1109/JSTARS.2017.2787650](https://doi.org/10.1109/JSTARS.2017.2787650)
- [2] L. Zhong, O. Kwoun, R. Rykhus, Interferometric Synthetic Aperture Radar (InSAR): Its Past, Present and Future, *Photogrammetric Engineering and Remote Sensing* 73-3 (2007), pp. 217-221.
- [3] M. G. D'Urso, V. Manzari, B. Marana, A combination of terrestrial laser-scanning point clouds and the thrust network analysis approach for structural modeling of masonry vaults, *Acta IMEKO* 10 (2021) 1, pp.257-264. DOI: [10.21014/acta_imeko.v10i1.1013](https://doi.org/10.21014/acta_imeko.v10i1.1013)
- [4] M. G. D'Urso, E. Corsi, C. Corsi, Mapping of archaeological evidences and 3D models for the historical reconstruction of archaeological sites, 2018 Metrology for Archaeology and Cultural Heritage (MetroArchaeo), Cassino, Italy, 22-24 October 2018. DOI: [10.1109/MetroArchaeo.43810.2018.9089783](https://doi.org/10.1109/MetroArchaeo.43810.2018.9089783)
- [5] D. M. Cobby, The use of airborne scanning laser altimetry for improved river flood prediction, PhD thesis, University of Reading.
- [6] M. Elmqvist, E. Jungert, F. Lantz, A. Persson, U. Soderman, Terrain modelling and analysis using laser scanner data in *International Archives of Photogrammetry and Remote Sensing*, 34(3/W4), 2001, pp. 219-226.
- [7] E. J. Huising, L. M. G. Pereira, Errors and accuracy estimates of laser data acquired by various laser scanning systems for topographic applications, *ISPRS Journal of Photogrammetry & Remote Sensing* 53 (1998), pp. 245-261. DOI: [10.1016/S0924-2716\(98\)00013-6](https://doi.org/10.1016/S0924-2716(98)00013-6)
- [8] K. Kraus, N. Pfeifer, Determination of terrain models in wooded areas with airborne laser scanner data, *ISPRS Journal of Photogrammetry & Remote Sensing* 53 (1998), pp. 193-203. DOI: [10.1016/S0924-2716\(98\)00009-4](https://doi.org/10.1016/S0924-2716(98)00009-4)
- [9] B. K. P.Horn, M. J. Brooks (editors), *Shape from Shading*, M.I.T. Press, Cambridge, Massachusetts, 1989. DOI: [10.1007/0-387-28831-7_23](https://doi.org/10.1007/0-387-28831-7_23)
- [10] K. Challis, P. Forlin, M. Kinsey, A generic toolkit for the visualization of archaeological features on airborne LiDAR elevation data, *Archaeol. Prospect* 18 (2011), pp. 279-289. DOI: [10.1002/arp.421](https://doi.org/10.1002/arp.421)
- [11] R. N. Hesse, LiDAR-derived Local Relief Models. A new tool for archaeological prospection, *Archaeological Prospect* 17 (2010), pp. 67-72. DOI: [10.1002/arp.374](https://doi.org/10.1002/arp.374)
- [12] R. Yokoyama, M. Sirasawa, R. J. Pike, Visualizing topography by openness: A new application of image processing to digital elevation models, *Photogramm. Eng. Remote Sensing* 68 (2002), pp. 257-265
- [13] Z. Kokalj, K. Zaksek, K. Ostir, Application of sky-view factor for the visualisation of historical landscape features in Lidar-derived relief models, in *Antiquity* 85 (327), pp. 263-273. DOI: [10.1017/S0003598X00067594](https://doi.org/10.1017/S0003598X00067594)

- [14] H. Van den Berghe, W. Gheyle, N. Note, B. Stichelbaut, M. Van Meirvenne, J. Bourgeois, V. Van Eetvelde, Revealing the preservation of First World War shell hole landscapes based on a landscape change study and LIDAR, *Journal of Geography*, (2018), pp. 1-14.
DOI: [10.1080/00167223.2018.1556105](https://doi.org/10.1080/00167223.2018.1556105)
- [15] I. Florinsky, Combined analysis of digital terrain models and remotely sensed data in landscape investigations, *Progress in Physical Geography* 22(1) (1998), pp. 33-60.
DOI: [10.1177/030913339802200102](https://doi.org/10.1177/030913339802200102)
- [16] I. Florinsky, An illustrated introduction to general geomorphometry, *Progress in Physical Geography* 41(6) (2017), pp. 1-30.
DOI: [10.1177/0309133317733667](https://doi.org/10.1177/0309133317733667)
- [17] W. Gheyle, B. Stichelbaut, T. Saey, N. Note, D. Hanssens, H. Van den Berghe, J. Bourgeois, Scratching the surface of war: airborne laser scans of the great war conflict landscape in Flanders (Belgium), *Applied Geography* 90 (2018), pp.55-68.
DOI: [10.1016/j.apgeog.2017.11.011](https://doi.org/10.1016/j.apgeog.2017.11.011)
- [18] C. Listopad, R. Masters, J. Drake, J. Weishampel, C. Branquinho, Structural diversity indices based on airborne LiDAR as ecological indicators for managing highly dynamic landscapes, *Ecological Indicators* 57 (2015), pp.268-279.
DOI: [10.1016/j.ecolind.2015.04.017](https://doi.org/10.1016/j.ecolind.2015.04.017)
- [19] L. Magnini, C. Bettineschi, A. De Guio, Object-based shell craters classification from LiDAR-derived sky-view factor, *Archaeological Prospection* 24(3)(2017), pp.211-223.
DOI: [10.1002/arp.1565](https://doi.org/10.1002/arp.1565)
- [20] C. Stal, J. Bourgeois, P. De Maeyer, G. de Mulder, A. de Wulf, R. Goossens, B. Stichelbaut, Kemmelberg (Belgium) case study: comparison of DTM analysis methods for the detection of relicts from the First World War, in *Remote Sensing for Science, Education and Natural and Cultural Heritage* (proceedings of the EARSel Symposium, Paris (2010), pp.65-71.
- [21] G. Bitelli, C. Balletti, R. Brumana, L. Barazzetti, M. G. D'Urso, F. Rinaudo, G. Tucci, Metric Documentation of Cultural Heritage: Research Directions from the Italian Gamher Project, in *The international archives of the photogrammetry, remote sensing and spatial information sciences, XLII-2/W5, 2017, 26th International CIPA Symposium Ottawa, Canada, 2017, PP.83-89.*
DOI: [10.5194/isprs-archives-XLII-2-W5-83-2017](https://doi.org/10.5194/isprs-archives-XLII-2-W5-83-2017)
- [22] M. G. D'Urso, C. L. Marino, A. Rotondi, On 3D dimension: study cases for archaeological sites, in *The international archives of the photogrammetry, remote sensing and spatial information sciences, XL-6, 2014, pp. 13-18, ISSN: 1682-1750.*
DOI: [10.5194/isprsarchives-XL-6-13-18](https://doi.org/10.5194/isprsarchives-XL-6-13-18)
- [23] M. Doneus, C. Briese, Airborne Laser Scanning in Forested Areas - Potential and Limitations of an Archaeological Prospection Technique, in *Remote Sensing for Archaeological Heritage Management: Proceedings of the 11th EAC Reykjavik, Iceland, March 2010.*
- [24] J. Aldrighettoni, (Great War)-scapes: a future for military heritage. The testimonial gradient as a new paradigm. PhD Thesis, Trento, 2022.
- [25] J. Aldrighettoni, The fortified system of the Doss Trento. Traces of militarization from the Napoleonic era to the Great War, *Sustainable Mediterranean Construction* 1 (2019), pp.63-70
- [26] J. Aldrighettoni, A. Quendolo, Warscape Biography: from Historical Air-photos to Lidar Data. The Revealing of the Great War's Permanences on the Contemporary Landscapes, *Journal of Physics: Conference Series*, v. 2204, 2022.
DOI: [10.1088/1742-6596/2204/1/012051](https://doi.org/10.1088/1742-6596/2204/1/012051)
- [27] J. Aldrighettoni, M. G. D'Urso, An interdisciplinary approach for unveiling and enhancing the first world war heritage in the landscape, in *ISPRS Annals of the Photogrammetry, Remote Sensing and Spatial Information, V-5-2022.*
DOI: [10.5194/isprs-annals-V-5-2022-17-2022](https://doi.org/10.5194/isprs-annals-V-5-2022-17-2022)
- [28] A. Quendolo, J. Aldrighettoni, Reading a militarized landscape. Themes and methodological approaches for the recognition of stratifications, in *Sustainable Mediterranean Construction* (Special Issue nr. 1), 2019.
- [29] J. Aldrighettoni, A. Quendolo, Warscapes: A Submerged Information Basin. The Contribution of LiDaR Data to the Unveiling, *Proc. of the 2020 IMEKO TC4 Int. Conf. on Metrology for Archaeology and Cultural Heritage, Trento, Italy, 22 - 24 October 2020, pp. 15-20. Online [Accessed 24 April 2023]*
<https://www.imeko.org/publications/tc4-Archaeo-2020/IMEKO-TC4-MetroArchaeo2020-004.pdf>
- [30] N. Poirier, F. Baleux, C. Calastrenc, The Mapping of Forested Archaeological Sites Using UAV LiDar: a feedback from a south-west France Experiment in Settlement & Landscape Archaeology, *ISTE OpenScience*, 2020, 24 pp.
DOI: [10.21494/ISTE.OP.2020.0556](https://doi.org/10.21494/ISTE.OP.2020.0556)
- [31] J. Fernàndex-Lozano, G. Gutiérrez-Alonso, Improving archaeological prospection using localized UAVs assisted photogrammetry: an example from the Roman Gold District of the Eria River Valley (NW Spain), *Journal Archeological Science* 5 (2016), pp. 509-520.
DOI: [10.1016/j.jasrep.2016.01.007](https://doi.org/10.1016/j.jasrep.2016.01.007)
- [32] C. Parcero-Oubiña, S. Niòn-Alvarez, Forms of settlement inequality over space. A GIS-based method for measuring differences among settlements, *Journal Archeological Science* 35 (2021), art. No. 102739.
DOI: [10.1016/j.jasrep.2020.102739](https://doi.org/10.1016/j.jasrep.2020.102739)
- [33] N. Fontana, La regione fortezza. Il sistema fortificato del Tirolo: pianificazione, cantieri e militarizzazione del territorio da Francesco I alla Grande Guerra, *Museo Storico Italiano della Guerra*, 2016. [In Italian]
- [34] S. Flaim, Restauro dei forti austroungarici trentini. Dal progetto Grande Guerra alla ricorrenza del centenario, in *Il recupero dei forti austroungarici trentini*, Trento, 2013. [In Italian]
- [35] S. Isgrò, Il sistema di fortificazione austro-ungarico nelle ricognizioni dello scacchiere orientale, storia, disegno e architettura nelle iconografie di viaggio degli ufficiali di Stato maggiore, *Aracne*, 2017. [In Italian]
- [36] W. R. Rosner, Fortificazione e operazione. Lo sbarramento degli altipiani di Folgaria, lavarone e Luserna, Trento, *Alcione Editore*, 2016. [In Italian]
- [37] G.M. Tabarelli, I forti austriaci nel Trentino e in Alto Adige, *Temi Editrice*, 1990. [In Italian]
- [38] D. Leoni, C. Zadra, La Grande Guerra. Esperienza, memoria, immagini. Bologna, 1986. [In Italian]
- [39] V. Jeschkeit, Trento 1915-1918 la città militarizzata. La sezione di difesa, *Curcu&Genovese*, 2016. [In Italian]
- [40] J. Aldrighettoni, The enhancement of the vestigia of the Great War through scenarios perspectives, in D. Fanzini, A. Tartaglia, R. Riva (a cura di) *Project challenges: sustainable development and urban resilience, Santarcangelo di Romagna (RN): Maggioli Editore*, 2019, ISBN: 9788891632487, p. 219-226.
- [41] R. De Matos Machado, J. P. Toumazet, J. C. Beres, J. P. Amat, A. J. Fassetta, F. Betard, C. Bilodeau, P. J. Hupy, S. Jacquemot, War landform mapping and classification on the Verdun battlefield (France) using airborne LiDAR and multivariate analysis in Earth surface process and landforms, 2019.
- [42] A. Mayoral, J. P. Toumazet, F. X. Simon, F. Vautier, J. L. Peiry, The Highest Gradient Model: A New Method for Analytical Assessment of the Efficiency of LiDAR-Derived Visualization Techniques for Landform Detection and Mapping, *Remote Sensing* 9(2), 2017.
DOI: [10.3390/rs9020120](https://doi.org/10.3390/rs9020120)
- [43] N. S. Anders, A. C. Seijmonsbergen, W. Bouten, Geomorphological Change Detection Using Object-Based Feature Extraction From Multi-Temporal LiDAR Data, in *IEEE Geoscience and Remote Sensing Letters* 10(6) (2013), pp. 1587-1591.
DOI: [10.1109/LGRS.2013.2262317](https://doi.org/10.1109/LGRS.2013.2262317)
- [44] M. C. Allen, T. Almqvist, C. T. Barreca, J. L. Lockwood, A lidar-based openness index to aid conservation planning for grassland wildlife, *Avian conservation and ecology* 17(1), 2022.
DOI: [10.5751/ACE-02078-170116](https://doi.org/10.5751/ACE-02078-170116)